

## Inverted many-body mobility edge in a central qudit problem

Saeed Rahamanian Koshkaki  and Michael H. Kolodrubetz 

Department of Physics, University of Texas at Dallas, Richardson, Texas 75080, USA



(Received 16 December 2020; accepted 2 February 2022; published 25 February 2022)

Many interesting experimental systems, such as cavity QED or central spin models, involve global coupling to a single harmonic mode. Out of equilibrium, it remains unclear under what conditions localized phases survive such global coupling. We study energy-dependent localization in the disordered Ising model with transverse and longitudinal fields coupled globally to a  $d$ -level system (qudit). Strikingly, we discover evidence for an inverted mobility edge where high-energy states are localized whereas low-energy states are delocalized. This prediction is supported by shift-and-invert eigenstate targeting and Krylov time evolution up to  $L = 13$  and 18, respectively. We argue for a critical energy of the localization phase transition which scales as  $E_c \propto L^{1/2}$ , consistent with finite-size numerics. We also show evidence for a reentrant many-body localization phase at even lower energies despite the presence of strong effects of the central mode in this regime. Similar results should occur in the central spin- $S$  problem at large  $S$  and in certain models of cavity QED.

DOI: [10.1103/PhysRevB.105.L060303](https://doi.org/10.1103/PhysRevB.105.L060303)

**Introduction.** Improvements in quantum control have brought nonequilibrium quantum systems to the forefront of condensed-matter and atomic, molecular, and optical physics. Novel phases of matter are possible out of equilibrium, most of which require many-body localization [1,2]. Many-body localization (MBL) results when sufficiently strong disorder prevents ergodicity in interacting systems and is the only known generic route to avoid thermal equilibrium in isolated quantum systems [3,4]. Most numerical and analytical claims of MBL rest upon the assumption of low-dimensional, locally interacting Hamiltonians, and sufficiently long-range nonconfining interactions are generally believed to destroy MBL [5–8].

It was, therefore, surprising when we recently found that MBL can survive coupling to a global degree of freedom [9]. Global coupling to a photon is a common occurrence in many-body cavity QED where the cavity mode is primarily used to create all-to-all interactions between the atoms. The key result of Ref. [9] was that the strength of this interaction is controlled by photon number in the cavity  $N$ . If one takes the number of atoms  $L$  to infinity whereas keeping the ratio  $N/\sqrt{L}$  fixed, all-to-all interactions remain sufficiently weak to allow an MBL phase.

This opens the interesting possibility that as the photon number—or, equivalently, the energy—is lowered, all-to-all interactions will reemerge and thermalize the system. This implies localization at high energies and thermalization at low energies, leading to an inversion of the conventional many-body mobility edge. In this Letter, we will confirm that prediction using numerical and analytical tools, further uncovering a reentrant MBL phase at even lower energies. Although similar phenomena occur in cavity QED, we argue that they are more favorable in nonbosonic models, such as the central spin- $S$  and central  $d$ -level systems (qudit).

**Model.** We start from the same Hamiltonian as Ref. [9], which was motivated by a standard model of spin-1/2 particles undergoing Floquet many-body localization [10]. In

the Floquet extended zone picture, the time-periodic drive is treated quantum mechanically by mapping it to a harmonic mode. This is represented geometrically in the inset to Fig. 1. The spins form a locally coupled chain with periodic boundary conditions. These spins all couple globally to a single degree of freedom, such as a cavity photon or central spin  $S$ . The goal of this Letter will be to study the low-energy limit where quantization of the central degree of freedom becomes important.

Specifically, our Hamiltonian can be written

$$H = \frac{H_+}{2} + \frac{H_-}{4}(\hat{a} + \hat{a}^\dagger) + \hat{n}\Omega, \quad (1)$$

where  $H_\pm = H_z \pm H_x$ ,

$$\begin{aligned} H_x &= \sum_{i=1}^L g\Gamma\sigma_i^x, \\ H_z &= \sum_{i=1}^L J\sigma_i^z\sigma_{i+1}^z + \sum_{i=1}^L (h + g\sqrt{1 - \Gamma^2}G_i)\sigma_i^z, \\ \hat{a}^\dagger &= \sum_{n=1}^{d-1} |n\rangle\langle n-1|, \quad \hat{n} = n \sum_{n=0}^{d-1} |n\rangle\langle n|, \end{aligned} \quad (2)$$

$\sigma_i^{x,z}$  are Pauli matrices, and  $G_i$  is a Gaussian random variable of zero mean and unit variance. Units are set by  $J = 1$ . The spin-1/2 Hamiltonians  $H_\pm$  yield static models with both MBL and thermal phases. The operators  $\hat{a}$  and  $\hat{n}$  play the role of lowering and number operators for the central mode. In this Letter, we mainly study the case of a central  $d$ -level system—a qudit—for which  $\hat{a}$  lowers the excitation number by one with the unit matrix element; this will be compared to photons and central spin  $S$  later in the Letter. The qudit levels are split by a bare energy  $\Omega$  (with  $\hbar = 1$ ) and can be excited through coupling to the spin Hamiltonian  $H_-$ . The most important parameter for localization is  $\Gamma$ , which controls both transverse field strength and disorder strength. For small  $\Gamma$  considered

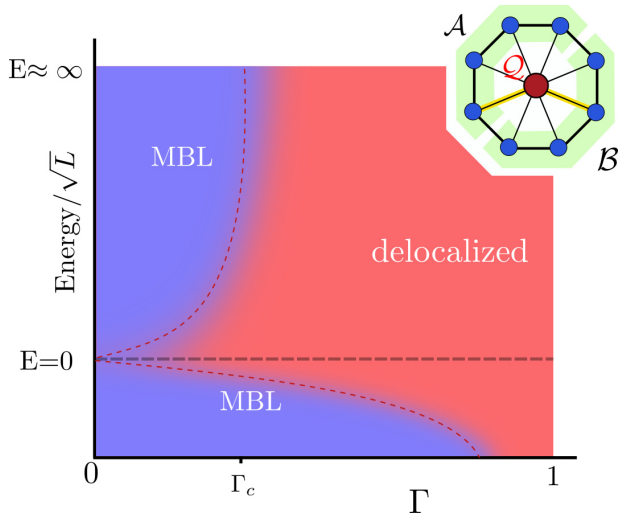


FIG. 1. Proposed phase diagram of inverted mobility edge for the Ising model in the presence of a global qudit or a spin- $S$  mode. For  $\Gamma < \Gamma_c \approx 0.33$ , we predict a delocalized to MBL phase transition as the energy is increased—an inverted mobility edge.

here, the dominant role is to add delocalizing quantum fluctuations both statically to the spin chain and via coupling to the central qudit. The limits  $\Gamma = 0$  and  $1$  represent trivially localized and thermalizing phases, respectively. Other parameters are chosen as  $g = 0.9045$ ,  $h = 0.809$ , and  $\Omega = 3.927$  based on previous work [9].  $\Omega$ , in particular, is chosen large but finite to enable nonresonant high-frequency expansions; the results are expected to apply for a generic such  $\Omega$ . We expect that our results will be independent of these particular parameters, although we note that MBL is generally favored by large  $\Omega$ . Furthermore, we will use  $d = 12$  throughout to approximate  $d = \infty$  such that only the lower cutoff on qudit number  $n \geq 0$  plays a role.

*Mobility edge.* In this model, Ref. [9] found evidence for an infinite-temperature phase transition ( $E \approx \text{tr}[H]/\text{tr}[1]$ ) between MBL at small  $\Gamma$  and thermalization at large  $\Gamma$  upon taking  $L \rightarrow \infty$  at finite  $d/\sqrt{L}$ . The transition occurs at  $\Gamma_c \approx 0.33$  for  $d/\sqrt{L} \gg 1$ , which corresponds to the Floquet limit. In this Letter, we will study the energy dependence of this transition. In order to obtain initial insight into energy dependence, we utilize the results of the high-frequency expansion [9], rederived in the Supplemental Material for clarity [11]. Physically, the high-frequency expansion (HFE) involves perturbatively eliminating fluctuations of the central mode via a canonical transformation, similar to the Floquet-Magnus expansion [12,13] or Schrieffer-Wolff transformation [14]. For  $d = \infty$ , this gives an effective Hamiltonian,

$$H_{\text{eff}} = \frac{H_+}{2} - \frac{(H_-)^2}{16\Omega} |0\rangle\langle 0| + \hat{n}\Omega + O(\Omega^{-2}).$$

The first term in  $H_{\text{eff}}$  consists of the undriven Hamiltonian  $H_+$ . The second term comes from the qudit raising and lowering operators, which commute with each other except at the edge of the spectrum (the state  $|0\rangle$ ). Physically, this means that for qudit states  $n > 0$ , virtual fluctuations in which the qudit number increases or decreases destructively interfere with each other, resulting in no change to the Hamiltonian at second

order. By contrast, in state  $|0\rangle$ , the qudit can only fluctuate up in number, resulting in a nonzero induced interaction  $\propto H_-^2/\Omega$  which, crucially, is only active when the qudit is at its extremal state  $|0\rangle$ . For our model, this gives infinite range interactions near the zero energy state, which compete with local interactions in  $H_+$  to thermalize the system. We note that this prediction is consistent with the conventional mobility edge found for an Anderson-localized system coupled to a central site [15] since for that case the effective central dimension was  $d = 2$  for which all states experience this thermalizing long-range term. Higher-order terms will give long-range interactions mediated by states  $|1\rangle$ ,  $|2\rangle$ , etc. but suppressed by powers of  $\Omega^{-1}$ .

The HFE suggests the existence of an inverted mobility edge. For high-energy  $E/\Omega \gg 1$  for which the qudit number is  $n \gg 1$ , no infinite-range interactions are produced, and the MBL-delocalized transition is given by that of the locally dressed  $H_+$  Hamiltonian with  $\Gamma_c \approx 0.33$ . For  $E \approx 0$  ( $n \approx 0$ ), infinite-range interactions compete with  $H_+$ , generically leading to thermalization.

*Numerics.* To distinguish the MBL and thermal phases numerically, we first study energy eigenstates of the Hamiltonian (1) using shift-and-invert methods [16] to target ten eigenstates near a given energy, up to a maximum system size of  $L = 13$ . Thermal systems are expected to be approximated by random matrices, whereas MBL systems are not. Looking at the energy levels, this implies that thermal eigenstates undergo level repulsion, following Wigner-Dyson level statistics, whereas MBL eigenstates follow Poisson level statistics with no level repulsion. This is captured by the level spacing statistic [17],

$$r_n = \frac{\min(\delta E_n, \delta E_{n+1})}{\max(\delta E_n, \delta E_{n+1})}, \quad (3)$$

where  $\delta E_n = E_n - E_{n-1}$  is the gap between ordered eigenenergies  $E_n$ . For Poisson statistics,  $\langle r_n \rangle \approx 0.386 \equiv r_{\text{Pois}}$ , whereas for the Gaussian orthogonal ensemble (GOE),  $\langle r_n \rangle \approx 0.53 \equiv r_{\text{GOE}}$ . Figures 2(a)–2(c) show the numerically calculated level statistics. At the largest  $L$ , states near  $E = 0$ , corresponding to the bare energy of the qudit ground-state  $|0\rangle$ , converge toward  $r_{\text{GOE}}$ . At both lower and higher energies, the level statistics appear Poissonian, suggesting that the system is localized. An approximate window for thermalization is sketched in the plots. We see that the level statistics converge towards the GOE value in this region. Interestingly, a reemergent MBL phase appears at low energies  $E < 0$ . This is consistent with the high-frequency expansion, which at low enough energies will be dominated by the term  $-(H_-)^2/(16\Omega)$ . Although this term has been argued to give infinite-range interactions that compete with short-range interactions, in isolation it shares eigenstates with the local Hamiltonian  $H_-$ . Therefore, MBL for  $E < 0$  apparently comes from the static MBL phase of  $H_-$ .

Full convergence to  $r_{\text{GOE}}$  is difficult to see, particularly, for small values of  $\Gamma$ . Therefore, we turn to the half-system mutual information and Kullback-Leibler divergence. The KLD measures similarity between eigenstates [18]. For each eigenstate  $|n\rangle$ , a probability distribution is defined by  $p_n(i) = |\langle i|n\rangle|^2$ , where  $|i\rangle$  is an element of the  $\sigma^z \otimes \hat{n}$  basis. For two

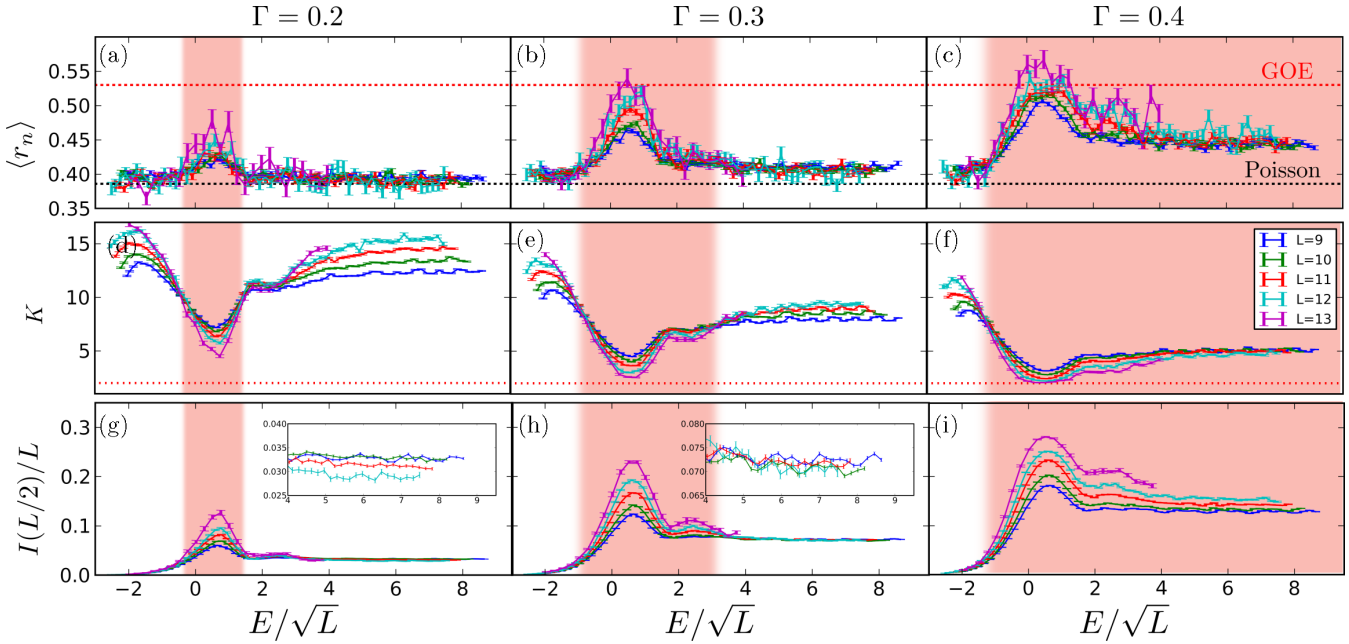


FIG. 2. Energy dependence of localization via three metrics: (a)–(c) level statistic  $\langle r_n \rangle$ , (d)–(f) Kullback-Leibler divergence (KLD), and (g)–(i) half-system mutual information  $I(L/2)$ . The shaded red color indicates the approximate region of delocalization, based on finite-size crossings of the KLD. The inset plots show magnification of  $I(L/2)/L$  for higher-energy data points.

neighboring energy eigenstates  $|n\rangle$  and  $|n+1\rangle$ , the KLD is defined by  $K = \sum_i^{\dim(H)} p_n(i) \ln \frac{p_n(i)}{p_{n+1}(i)}$ . In the MBL phase, this quantity increases linearly with system size  $\propto \ln [\dim(H)]$  because nearby eigenstates are completely uncorrelated. For the thermal phase, one expects  $K = 2$  in the thermodynamic limit from random matrix theory [18]. The energy-dependent KLD is shown in Figs. 2(d)–2(f). The KLD of the thermal phase is notably lower than MBL phase and for small  $\Gamma$  shows an inversion of the finite-size dependence;  $K$  increases with system size in the MBL phase and decreases with system size in the delocalized phase. A finite-size crossing of the KLD gives an approximate location of the delocalized phase, which is seen to increase for increasing  $\Gamma$ .

Similar behavior is seen in the half-system mutual information of the energy eigenstates, defined as

$$I(L/2) \equiv I(A, B) = S(A) + S(B) - S(A \cup B), \quad (4)$$

where  $S(A) = -\text{tr}[\rho_A \ln(\rho_A)]$  is the von Neumann entanglement entropy of subsystem  $A$ . The system is split into three pieces as shown in the inset to Fig. 1, where  $A$  and  $B$  correspond to dividing the spin system into halves and  $S(A \cup B) = S_q$  is the entanglement entropy of the qudit. Mutual information is chosen to best capture entanglement between the subsystems  $A$  and  $B$ , which should be area law in the MBL phase and volume law in the delocalized phase [19]. As seen in Figs. 2(g)–2(i), mutual information is indeed higher in the delocalized phase, although the apparent super-volume-law scaling is a finite-size effect which is expected to go away at larger system sizes [9,20]. Note that the mutual information remains well below its maximal (Page) value of  $I(L/2) \rightarrow L \ln(2) \approx 0.693L$ , further demonstrating the large finite-size effects.

To approach larger system sizes up to  $L = 18$ , we use Krylov time evolution [16], which is limited to shorter times. For the localized phase, we expect the system to retain memory of its initial state to an exponentially long time, resulting in a quick plateau of the mutual information, followed by slow—potentially logarithmic—growth [21,22]. By contrast, ergodic phases should quickly reach thermal equilibrium with much larger entanglement. The crossover behavior is more complicated, but physics deep in these phases should be well approximated by this simple picture.

We studied time evolution by preparing initial product states in the  $\sigma^z \otimes \hat{n}$  basis and evolving the wave function using the Krylov method [23]. We initialized these states within a given energy window of width  $\Delta E = 0.2$ . Fig. 3 shows energy-resolved mutual information. We are not able to obtain data for sufficiently long times to clearly identify a late-time plateau, but points within the MBL and delocalized regions show different trends. For delocalized values of  $E/\sqrt{L} = 0.5$ , the mutual information approaches a plateau value near the theoretical maximum  $I(L/2) = L \ln(2)$ . On the other hand, for the states near the ground state and in the middle of the spectrum, data consistent with a logarithmic growth of mutual information is detected, which is suggestive of localization in the thermodynamic limit [21,22]. Taking the instantaneous mutual information at late-time  $t = 3900$ , we observe the same trend as the data obtained using energy eigenstates (top panel of Fig. 3).

Finally, we note that, in our model, the qubit ground state is at  $E = 0$ , and all excited states are at  $E = n\Omega$ . Unlike other words that are symmetric around  $E = 0$  [9,24], our model has no such symmetric energy spectrum.

*Discussion.* Our data are consistent with the picture from the high-frequency expansion suggesting an inverted mobility edge for  $\Gamma < \Gamma_c$ . A concern for this analysis is the fact that

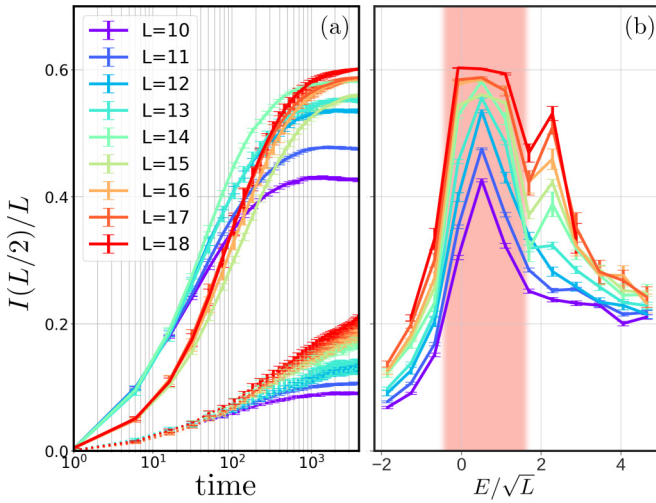


FIG. 3. (a) Dynamics of  $I(L/2)$  obtained using Krylov time evolution starting from a product state. The dashed curves correspond to the MBL regime ( $E/\sqrt{L} = -1.26 \pm 0.024$ ), and the solid lines correspond to the delocalized regime ( $E/\sqrt{L} = 0.51 \pm 0.024$ ). (b) Energy dependence of  $I(L/2)$  at late times,  $t = 3900$ . All data are for  $\Gamma = 0.3$ . In this plot, the finite-size effect is strong as going from  $L = 14$  to  $L = 15$  the form of the logarithm plot changes significantly.

the HFE is asymptotic rather than convergent for  $L = \infty$  and finite  $\Omega$  [25]. Therefore, we numerically compare the results from the exact numerics to those from the HFE. The HFE matches very well in the low-energy reemergent MBL phase and appears to approach the correct answer in the high-energy phase where convergence is expected when the system is localized by standard arguments for Floquet MBL [26,27]. Unsurprisingly, the HFE does not converge in the thermal regime, which is a signature of resonant delocalization [11].

The HFE also shows why inverted mobility edges are more apparent with central qudits or spins than with bosonic modes. In the photonic HFE, the leading long-range interactions become  $-(H_-)^2/\Omega$  independent of photon number [11]. Higher-order corrections will pick up photon number dependence but are more difficult to see due to the  $\Omega^{-r}$  suppression at  $r$ th order. For a central spin  $S$ , the relevant commutator is  $[S^-, S^+] = -2S^z$ , which becomes large at the edges of the spin spectrum (large  $|S^z|$ ), similar to the qudit and, thus, will also show an inverted mobility edge as seen in the Supplemental Material [11]. In general, the energy dependence of localization will depend on the manner in which the photon couples to the many-body system, and similar HFEs should enable analysis of the energy dependence.

We can also get some insight from the HFE about the energy at which the MBL-delocalized transition occurs. Within the HFE, the density of states for each qudit level  $|n\rangle$  is approximately Gaussian with mean  $n\Omega$  and width  $\sim J\sqrt{L}$ . From the HFE, only states from the  $n = 0$  branch contribute to the infinite-range thermalizing interactions at leading order. Since the energy window corresponding to  $n = 0$  extends up to

$E_0 \approx J\sqrt{L}$ , we postulate that the critical energy will scale similarly:  $E_c \propto L^{1/2}$ . We are unable to definitively confirm this scaling given our small finite-size numerics. However, plotting data as a function of  $E/\sqrt{L}$ —as is performed throughout the Letter—appears to give better data collapse than plotting as a function of  $E$  (see the Supplemental Material [11]).

Experimentally, a few systems exist in which a nonbosonic central mode is globally coupled to an interacting spin or electron system as required for this physics. A notable example is the recent realization of a cavity QED-like architecture with superconducting qubits playing the role of mirrors [28,29]. The cavity mode is replaced by the dark state manifold of a qubit chain, whose raising and lowering operators satisfy the commutation relations of large spin  $S$  [11]. The size of this spin is controllable by the number of qubits in the chain, and hence can be scaled to large values as we use here. Currently, experiments have shown coupling of the dark mode to a single atomlike qubit to simulate cavity QED, but we expect that coupling to a disordered interacting spin chain is practical through conventional superconducting qubit architectures [30]. Similar large-spin algebra results for coupling between polaritons in a semiconductor microcavity and spin impurities in the semiconductor since in certain regimes the polaritons “inherit” the nonbosonic commutation relations of their matter component [31,32]. Finally, we note that, for generic cavity-atom coupling in conventional cavity QED we also expect an inversion of the mobility edge in certain regimes, as will be detailed in an upcoming paper [33].

To summarize we have shown that in centrally coupled spin chains, such as those with a central qudit or spin  $S$  in a magnetic field, an inversion of the many-body mobility edge is possible. Although a similar inversion has been predicted in other scenarios [34,35], the mechanism here is fundamentally different, relying on infinite-range interactions induced by a central mode. We postulate that an inversion of the mobility edge will be a generic feature of many such models since long-range thermalizing interactions are most strongly induced at the edge of the spectrum where the finiteness of the central mode becomes apparent. This phenomenology opens up further intriguing questions about localization in such systems with competition between local and global interactions, such as the existence and character of localized bits ( $\ell$ -bits [36,37]). Furthermore, as the energy-dependent phase transition comes from global interactions, it should be in a different class than recent avalanche pictures of the MBL transition [38–41].

**Acknowledgments.** We would like to acknowledge useful discussions with R. Nandkishore, N. Ng, A. Polkovnikov, E. Rabani, M. Thoss, and S. Wenderoth. This work was performed with support from the National Science Foundation through Award No. DMR-1945529 and the Welch Foundation through Award No. AT-2036-20200401. We used the computational resources of the Lonestar 5 cluster operated by the Texas Advanced Computing Center at the University of Texas at Austin and the Ganymede and Topo clusters operated by the University of Texas at Dallas’ Cyberinfrastructure & Research Services Department.

[1] J. R. Wootton and J. K. Pachos, *Phys. Rev. Lett.* **107**, 030503 (2011).

[2] D. A. Huse, R. Nandkishore, V. Oganesyan, A. Pal, and S. L. Sondhi, *Phys. Rev. B* **88**, 014206 (2013).

[3] R. Nandkishore and D. A. Huse, *Annu. Rev. Condens. Matter Phys.* **6**, 15 (2015).

[4] D. A. Abanin, E. Altman, I. Bloch, and M. Serbyn, *Rev. Mod. Phys.* **91**, 021001 (2019).

[5] R. M. Nandkishore and S. L. Sondhi, *Phys. Rev. X* **7**, 041021 (2017).

[6] N. Y. Yao, C. R. Laumann, S. Gopalakrishnan, M. Knap, M. Müller, E. A. Demler, and M. D. Lukin, *Phys. Rev. Lett.* **113**, 243002 (2014).

[7] P. Ponte, C. R. Laumann, D. A. Huse, and A. Chandran, *Philos. Trans. R. Soc. A* **375**, 20160428 (2017).

[8] D. Hetterich, N. Y. Yao, M. Serbyn, F. Pollmann, and B. Trauzettel, *Phys. Rev. B* **98**, 161122(R) (2018).

[9] N. Ng and M. Kolodrubetz, *Phys. Rev. Lett.* **122**, 240402 (2019).

[10] L. Zhang, V. Khemani, and D. A. Huse, *Phys. Rev. B* **94**, 224202 (2016).

[11] See Supplemental Material at <http://link.aps.org/supplemental/10.1103/PhysRevB.105.L060303> for details of the HFE, a numerical comparison between the HFE and the exact Hamiltonian, results for large- $S$  central spin models, and more details on potential experimental realizations.

[12] M. Bukov, L. D’Alessio, and A. Polkovnikov, *Adv. Phys.* **64**, 139 (2015).

[13] N. Goldman and J. Dalibard, *Phys. Rev. X* **4**, 031027 (2014).

[14] M. Bukov, M. Kolodrubetz, and A. Polkovnikov, *Phys. Rev. Lett.* **116**, 125301 (2016).

[15] D. Hetterich, M. Serbyn, F. Domínguez, F. Pollmann, and B. Trauzettel, *Phys. Rev. B* **96**, 104203 (2017).

[16] F. Pietracaprina, N. Macé, D. J. Luitz, and F. Alet, *SciPost Phys.* **5**, 45 (2018)..

[17] V. Oganesyan and D. A. Huse, *Phys. Rev. B* **75**, 155111 (2007).

[18] D. J. Luitz, N. Laflorencie, and F. Alet, *Phys. Rev. B* **91**, 081103(R) (2015).

[19] A. Pal and D. A. Huse, *Phys. Rev. B* **82**, 174411 (2010).

[20] N. Ng, S. Wenderoth, R. R. Seelam, E. Rabani, H.-D. Meyer, M. Thoss, and M. Kolodrubetz, *Phys. Rev. B* **103**, 134201 (2021).

[21] M. Serbyn, Z. Papić, and D. A. Abanin, *Phys. Rev. Lett.* **110**, 260601 (2013).

[22] J. H. Bardarson, F. Pollmann, and J. E. Moore, *Phys. Rev. Lett.* **109**, 017202 (2012).

[23] M. Brenes, V. K. Varma, A. Scardicchio, and I. Girotto, *Comput. Phys. Commun.* **235**, 477 (2019).

[24] C. R. Laumann, A. Pal, and A. Scardicchio, *Phys. Rev. Lett.* **113**, 200405 (2014).

[25] P. Weinberg, M. Bukov, L. D’Alessio, A. Polkovnikov, S. Vajna, and M. Kolodrubetz, *Phys. Rep.* **688**, 1 (2017).

[26] A. Lazarides, A. Das, and R. Moessner, *Phys. Rev. Lett.* **115**, 030402 (2015).

[27] P. Ponte, Z. Papić, F. Huvaneers, and D. A. Abanin, *Phys. Rev. Lett.* **114**, 140401 (2015).

[28] M. Mirhosseini, E. Kim, X. Zhang, A. Sipahigil, P. B. Dieterle, A. J. Keller, A. Asenjo-Garcia, D. E. Chang, and O. Painter, *Nature (London)* **569**, 692 (2019).

[29] A. Albrecht, L. Henriet, A. Asenjo-Garcia, P. B. Dieterle, O. Painter, and D. E. Chang, *New J. Phys.* **21**, 025003 (2019).

[30] Y. Chen, C. Neill, P. Roushan, N. Leung, M. Fang, R. Barends, J. Kelly, B. Campbell, Z. Chen, B. Chiaro, A. Dunsworth, E. Jeffrey, A. Megrant, J. Y. Mutus, P. J. J. O’Malley, C. M. Quintana, D. Sank, A. Vainsencher, J. Wenner, T. C. White, M. R. Geller, A. N. Cleland, and J. M. Martinis, *Phys. Rev. Lett.* **113**, 220502 (2014).

[31] G. F. Quinteiro, J. Fernández-Rossier, and C. Piermarocchi, *Phys. Rev. Lett.* **97**, 097401 (2006).

[32] M. J. Hartmann, F. G. Brandao, and M. B. Plenio, *Nat. Phys.* **2**, 849 (2006).

[33] R. Ge, S. R. Koshkaki, and M. H. Kolodrubetz (unpublished).

[34] W. De Roeck and F. Huvaneers, *Commun. Math. Phys.* **332**, 1017 (2014).

[35] M. Pino, L. B. Ioffe, and B. L. Altshuler, *Proc. Natl. Acad. Sci. USA* **113**, 536 (2016).

[36] M. Serbyn, Z. Papić, and D. A. Abanin, *Phys. Rev. Lett.* **111**, 127201 (2013).

[37] D. A. Huse, R. Nandkishore, and V. Oganesyan, *Phys. Rev. B* **90**, 174202 (2014).

[38] L. Zhang, B. Zhao, T. Devakul, and D. A. Huse, *Phys. Rev. B* **93**, 224201 (2016).

[39] A. Goremykina, R. Vasseur, and M. Serbyn, *Phys. Rev. Lett.* **122**, 040601 (2019).

[40] A. Morningstar and D. A. Huse, *Phys. Rev. B* **99**, 224205 (2019).

[41] N. Macé, F. Alet, and N. Laflorencie, *Phys. Rev. Lett.* **123**, 180601 (2019).